FOOD WEB CHAOS WITHOUT SUBCHAIN OSCILLATORS

BRIAN BOCKELMAN & BO DENG

ABSTRACT. A basic food web of 4 species is considered, of which there is a bottom prey X, two competing predators Y, Z on X, and a super predator W only on Y. The main finding is that population chaos does not require the existence of oscillators in any subsystem of the web. This minimum population chaos is demonstrated by increasing the relative reproductive rate of Z alone without alternating any other parameter nor any nullcline of the system. It occurs as the result of a period-doubling cascade from a Hopf bifurcation point. The method of singular perturbation is used to determine the Hopf bifurcation involved as well as the parameter values.

1. INTRODUCTION

The development of chaos theory has always intertwined with complex population dynamics since its inception. The question of under what minimum circumstance can chaos arise in population models was raised in [26] which postulates that it requires at the minimum the coupling of two oscillators from some shorter predator-prey chains. The main objective of this paper is to show that this hypothesis is false for a food web of four species in which chaos can occur even though none of the subchains contains any oscillator.

This paper also aims to address another important issue in population dynamics — the Competition Exclusion Principle ([16, 2, 31, 18]), which states that for most systems where two predators feed on a prey there cannot be any stable coexisting state. This principle has recently been shown not to hold for models at the stoichiometry level where nutrient limitation on growth is a factor (see [19]). It does not apply to such a 3-species competitive web mediated by an additional super-predator as shown in [1] (see also [17]). The same 4-species model is considered both in [1] and in this paper. Both lead to the same conclusion of competition inclusion coexistence in chaotic dynamics. However the main difference lies in whether the corresponding chaos is more or less likely to occur in real systems. For the dynamics of [1], part of the chaotic attractor lies precariously close to some species extinction zones because of the particularity of the mathematical construction via singular perturbation. For the chaotic dynamics considered here however, it stays considerably far away from these extinction edges, giving a greater plausibility to be observed in real systems.

Another novel point of this paper is worth mentioning. The prototypical chaos of the logistic map $x \mapsto \lambda x(1-x)$ ([21]) is resulted from changes in the intrinsic growth rate λ. This phenomenon of prolificacy generated chaos has not been observed previously in continuous population models. The chaos observed in this paper is indeed of this type, when only the relative intrinsic growth rate of one competitor varies while all other parameters remain fixed. More interestingly, it takes place even with all the underpinning structures in nullclines remain unchanged throughout the prolificacy enhanced route to chaos.

The chaotic dynamics found in this paper is not by an exclusive singular perturbation construction as with the case of [1]. Instead, it is found by a combination of singular perturbation analysis, Hopf bifurcation analysis, and a numerical bifurcation study on a period-doubling cascade originated from the Hopf point. Understanding the system mechanism that creates this phenomenon is particularly challenging because it seems that the singular perturbation approach alone is not thoroughly effective, unlike previous successes of the method ([7, 8, 9, 10, 1]).

The paper is organized as follows. Due to the complexity of the problem, a significant amount of nontechnical but essential background information from [1] is incorporated into to the first 5 sections. In particular, Section 2 gives an overview of the food web model considered. Section 3 reviews the techniques used, particularly the singular perturbation analysis, including the phenomenon of Pontryagin's delay of loss of stability. Sections 4 and 5 set up the framework, in particular, the set of conditions for the result. Section 6 presents the Hopf bifurcation result, and Section 7 the numerical simulation that leads to the chaotic dynamics. In many places of this paper, two points of view are presented — a biological one and a purely mathematical one. This is done to demonstrate not only the realism of the model but also a holistic alternative to the technical mathematics required. For example, although it is technically correct to state 'the derivative of the per-capita growth rate of X with respect to Y is negative', a paraphrase such as 'an increase in predators causes the prey's per-capita growth rate to decline' may be more preferable to a biologically inclined mind. Either way, the two statements are equivalent.

2. Description of the Model

For the mathematical model considered, let the population densities be X for the prey, Y, Z for the competing predators of the common prey X, and W for the top-predator on Y. We will assume that X is governed by Verhulst's logistic growth principle ([29, 20, 30]) in the absence of the predators, and all predators governed by Holling's Type II predation functional form ([14]), two of the most fundamental modelling principles in ecology. Under the assumption that there are no other forms of competition between Y, Z, the dimensional model is as follows

$$\left\{\begin{array}{l} \dfrac{dX}{dt} = rX\left(1-\dfrac{X}{K}\right) - \dfrac{p_1 X}{H_1+X}Y - \dfrac{p_2 X}{H_2+X}Z \\ \dfrac{dY}{dt} = \dfrac{b_1 p_1 X}{H_1+X}Y - d_1 Y - \dfrac{p_3 Y}{H_3+Y}W \\ \dfrac{dZ}{dt} = \dfrac{b_2 p_2 X}{H_2+X}Z - d_2 Z \\ \dfrac{dW}{dt} = \dfrac{b_3 p_3 Y}{H_3+Y}W - d_3 W \end{array}\right. \tag{1}$$

Here r is the intrinsic growth rate and and K is the carrying capacity for the prey. Parameter p_1 is the maximum predation rate per predator Y and H_1 is the semi-saturation density for which when $X = H_1$ the Y's predation rate is half of its maximum, $p_1/2$. Parameter b_1 is predator Y's birth-to-consumption ratio and d_1 is its per-capita death rate. The remaining parameters have parallel and analogous meanings.

As a necessary first step for mathematical analysis, we non-dimensionalize Eq.(1) so that the scaled system contains a minimum number of parameters. It also has the advantage for

uncovering equivalent dynamical behaviors with changes in different dimensional parameters. Using the same scaling ideas of [7] and the following specific substitutions for variables and parameters

$$
\begin{aligned}
&t \to b_1 p_1 t, \quad x = \frac{X}{K}, \quad y = \frac{Y}{Y_0}, \quad z = \frac{Z}{Z_0}, \quad w = \frac{W}{W_0} \\
&Y_0 = \frac{rK}{p_1}, \quad Z_0 = \frac{rK}{p_2}, \quad W_0 = \frac{b_1 p_1 Y_0}{p_3} \\
&\zeta = \frac{b_1 p_1}{r}, \quad \epsilon_1 = \frac{b_2 p_2}{b_1 p_1}, \quad \epsilon_2 = \frac{b_3 p_3}{b_1 p_1} \\
&\beta_1 = \frac{H_1}{K}, \quad \beta_2 = \frac{H_2}{K}, \quad \beta_3 = \frac{H_3}{Y_0} \\
&\delta_1 = \frac{d_1}{b_1 p_1}, \quad \delta_2 = \frac{d_2}{b_2 p_2}, \quad \delta_3 = \frac{d_3}{b_3 p_3},
\end{aligned} \tag{2}
$$

Eq.(1) is changed to this dimensionless form:

$$
\begin{cases}
\zeta \dfrac{dx}{dt} = x\left(1 - x - \dfrac{y}{\beta_1 + x} - \dfrac{z}{\beta_2 + x}\right) := x f(x,y,z) \\
\dfrac{dy}{dt} = y\left(\dfrac{x}{\beta_1 + x} - \dfrac{w}{\beta_3 + y} - \delta_1\right) := y g(x,y,w) \\
\dfrac{dz}{dt} = \epsilon_1 z\left(\dfrac{x}{\beta_2 + x} - \delta_2\right) := z h(x) \\
\dfrac{dw}{dt} = \epsilon_2 w\left(\dfrac{y}{\beta_3 + y} - \delta_3\right) := w k(y)
\end{cases} \tag{3}
$$

We refer to [1] for an ecological interpretation of the scaled dimensionless parameters. However, we need to emphasize the following that parameters, $1/\zeta, \epsilon_1, \epsilon_2$, are the maximum growth rates of X, Z, W relative to Y, refereed to as the XY-prolificacy, ZY-prolificacy, and the WY-prolificacy respectively. By the theory of allometry ([4, 5]), these ratios correlate reciprocally well with the 4th roots of the ratios of X, Z, W's body masses to that of Y's. Thus they may be of order 1 when predator's and prey's body masses are comparable or of smaller order if, as in plankton-zooplankton-fish, and most plant-herbivore-carnivore chains, the body masses are progressively becoming heavier in magnitude so that ζ and ϵ_2 are small parameters. In any case, a given web will find its corresponding prolificacy characteristics in parameters ζ, ϵ_i which are now isolated in plain view in Eq.(3). The main result of this paper is about the bifurcation of the system with the ZW-prolificacy parameter ϵ_1/ϵ_2 with all others fixed.

3. Notation and Singular Perturbation Method

To fix ideas and techniques, consider the xy-subsystem of (3) in the absence of the competitor z ($z = 0$) and the top-predator w ($w = 0$):

$$
\zeta \frac{dx}{dt} = x\left(1 - x - \frac{y}{\beta_1 + x}\right), \quad \frac{dy}{dt} = y\left(\frac{x}{\beta_1 + x} - \delta_1\right). \tag{4}
$$

It is singularly perturbed if $0 < \zeta \ll 1$. Variable y is the slow variable and the equation with $\zeta = 0$, $0 = x f(x,y,0)$ together with $dy/dt = y g(x,y,0)$, is the slow subsystem. It is a 1-dimensional equation on the slow manifold $0 = f(x,y,0)$ and $x = 0$. The curve $f(x,y,0) = 0$ is referred to as the nontrivial x-nullcline as opposed to the trivial x-nullcline $x = 0$. Variable

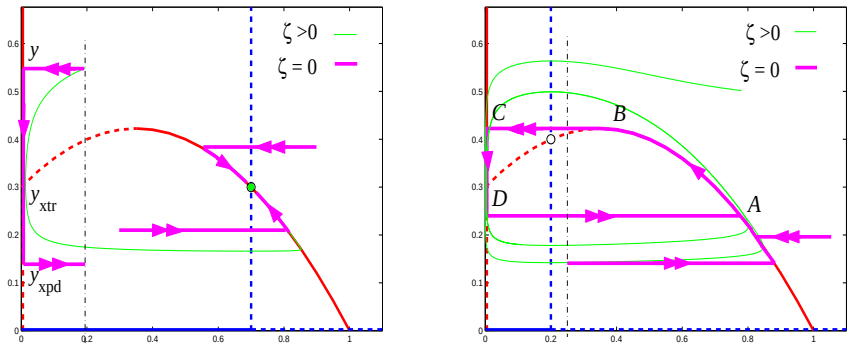

FIGURE 1. (a) Typical singular orbits in the case of stable xy-equilibrium state for which $x_{\rm xfd} < x_{\rm ynl} < 1$. See text for the derivation of $y_{\rm xpd}$ on the phenomenon of Pontryagin's delay of loss of stability at which a boom in x population occurs although the recovery starts after its crossing the dashed threshold on the parabolic x-nullcline near $y_{\rm xtr}$. (b) A typical singular orbit in limit cycle and its relaxed cycle for $0 < \zeta \ll 1$ in the case $0 < x_{\rm ynl} < x_{\rm xfd}$.

x is the fast variable and its equation with y frozen is the fast subsystem. More specifically, the fast subsystem is obtained by first rescaling the time $t/\zeta \to t$ to cast the system as $\dot{x} = xf(x,y,0),\ \dot{y} = \zeta y g(x,y,0)$ and then setting $\zeta = 0$ to get $\dot{x} = xf(x,y,0), \dot{y} = 0$ for which y is frozen as a parameter, and the equilibrium states are given by the x-nullcline, $0 = xf(x,y,0)$.

Fig.1(a,b) illustrate some essential elements of the singularly perturbed equations. Horizontal phase lines are fast orbits of the x-equation. Oriented curves on the x-nullclines are slow orbits. The directions of the these orbits are determined by their corresponding directional fields. More specifically, the nontrivial x-nullcline $0 = f(x,y,0)$ is typically a parabola-like curve with a maximal vertex. Point $(1,0)$ in it corresponds to the x-carrying capacity in the absence of the predator y. As y increases, the capacity continues but decreases. Thus the branch between the maximal point, denoted by $(x_{\rm xfd}, y_{\rm xfd})$, and $(1,0)$ is referred to as the predator-adjusted carrying capacity, which satisfies analytically $f(x,y,0) = 0, f_x(x,y,0) < 0$. It is stable for the x-equation, attracting fast orbits nearby. The maximum point is called the x-crash-fold point because for y immediately above it the fast x-solution always tends to the extinction branch $x = 0$. Mathematically, the x-equation undergoes a saddle-node bifurcation at the crash-fold point as y changes. The remaining branch between $(0, y_{\rm xtr})$ and the crash-fold is unstable for the fast x-equation. It represents the predator mediated threshold in x. Specifically, for a fixed y, the corresponding threshold value in x satisfies that above it the prey grows to its predator-adjusted capacity and below it the prey goes to extinction. As y increases the threshold in x increases whereas the capacity in x decreases, both coalescing at the crash-fold point.

Typical slow orbits always move down on the depleted resource branch $x = 0$ and down or up on the capacity branch $f(x,y,0) = 0$ depending on whether the resource amount x is smaller or larger than $x_{\rm ynl}$, as in the y-nullcline $x = x_{\rm ynl}$, that is a required minimum to sustain predator's growth since the per-capita rate $g(x,y,0) > 0$ only if the prey supply is sufficient $x > x_{\rm ynl}$.

A few concepts will be used throughout the paper. Predator y is said to be *efficient* (or *predatory efficient*) if it can make the predator-induced prey capacity equilibrium $f(x, y, 0) = 0$ to develop a crash-fold point $x_{\rm xfd} = (1 - \beta_1)/2 > 0$, namely $0 < H_1/K = \beta_1 < 1$. This means that the predator is able to reach half of its maximum predation rate at a prey density H_1 smaller than the prey's carrying capacity. Predator y is said to be *strong* if it is predatory efficient and can actually crash the prey. That is, at the crash-fold state $(x_{\rm xfd}, y_{\rm xfd})$ the predator can grow in per-capita: $g(x_{\rm xfd}, y_{\rm xfd}, 0) > 0$, which is solved as $x_{\rm xfd} = (1 - \beta_1)/2 > \beta_1\delta_1/(1 - \delta_1) = x_{\rm ynl}$. It is easy to see that the predator's relative mortality rate δ_1 should be relatively small as part of the requirement for the predator to be strong besides being efficient. Predator y is said to be *weak* if it is not strong.

A notation convention will be adopted throughout the paper. Presented by example, $x_{\rm xfd}$ means the x-coordinate of the fold point on the x-nullcline, and $y_{\rm xfd}$ is the y-coordinate of the same point. Thus $x_{\rm ynl}$ is the x-coordinate for the y-nullcline.

Another type of points that is critical to the analysis of singular perturbation is the transcritical point. For the fast x-equation, it is the intersection of the trivial and nontrivial branches of the nullcline, $(0, y_{\rm xtr})$. Above the point the extinction branch x is stable and below it it is unstable. Because of it an important phenomenon occurs, referred to as *Pontryagin's delay of loss of stability* ([25, 28]). It deals with the manner by which fast singular orbits jump away from the unstable trivial branch of the prey nullclines. In practical terms, the predator declines in a dire situation of depleted prey $x = 0$, followed by a surge in the prey's recovery after the predator reaches a sufficiently low density $y_{\rm xpd}$ to allow it to happen. The mathematical question is how the criticality $y_{\rm xpd}$ is determined. More specifically, let $(x_\zeta, y_\zeta)(t)$ be a solution to the perturbed equation with $\zeta > 0$ and an initial (x_0, y_0) satisfying $0 < x_0 < x_{\rm xfd}$ and y_0 above the threshold (Fig.1). In the singular limit $\zeta = 0$, the orbit converges to a concatenation of 2 fast orbits and 1 slow orbit. The first fast orbit lies on $y = y_0$, and the second lies on $y = y_{\rm xpd}$. According to the theory (see [1] for a derivation), the critical amount $y_{\rm xpd}$ that allows x to recover is determined by the following integral equation:

$$\int_{y_{\rm xpd}}^{y_0} \frac{f(0, s, 0)}{sg(0, s, 0)} ds = 0.$$

By substituting $s = y(t), y(0) = y_0$, the slow orbit on the trivial branch $x = 0$, and observing that $ds/(sg(0, s, 0)) = dt$, the equation changes to $\int_{T_{\rm xpd}}^0 f(0, y(t), 0)dt = 0$ where $T_{\rm xpd}$ is the corresponding duration of flight $y(T_{\rm xpd}) = y_{\rm xpd}$. Because f is the per-capita growth rate of the prey which has opposite signs around the transcritical point $y_{\rm xtr}$, and because the integral of f represents the accumulative per-capita growth rate during the transition, this equation simply means that the Pontryagin's delay of loss of stability (PDLS) point $y_{\rm xpd}$ is such that prey's accumulative per-capita growth rate over the growing phase $y < y_{\rm xtr}$ cancels it out over the declining phase $y > y_{\rm xtr}$. The PDLS point $y_{\rm xpd}$ depends on the initial y_0 which will be taken as the crash point $y_{\rm xfd}$ most of the times. The case illustrated is for the type of transcritical points at which the fast variable goes through a phase of crash-recovery-outbreak. All the known PDLS cases of our $XYZW$-model are of the crash-recovery-outbreak type.

Finally, the singular limit cycle $ABCD$ in Fig.1(b) has B the crash-fold point and D the PDLS point. It exists only if the predator can still grow at the crash-fold point ($x_{\text{ynl}} < x_{\text{xfd}}$). We point out that the singular cycle in the case of Fig.1(b) and the equilibrium point in the case of Fig.1(a) will all persist for small $0 < \zeta \ll 1$ because of their hyperbolicity. A proof of this fact as well as additional expositions on the geometric method of singular perturbations can be found in the literature, see [25, 24, 12, 11, 28, 3, 22, 6, 7, 18].

4. Preliminary Conditions

Although reducing the system to its dimensionless form greatly reduces the number of parameters, the resulting parameter space is still too large to be reasonably manageable. Therefore, we will impose a set of conditions to define the parameter region and consequently the dynamical structure considered.

Condition 1. *The chain prolific diversification condition: the maximum per-capita growth rates decrease from the bottom to the top along a food chain, and the differences between the rates are drastic:*

$$0 \ll b_3p_3 \ll b_1p_1 \ll r, \text{ equivalently, } 0 < \epsilon_2 \ll 1 \ll \frac{1}{\zeta}.$$

We note that this condition was referred to as 'trophic time diversification hypothesis' in [23, 7]. It means that the birthrate of the prey is much higher than that of the competitor Y, and that the birthrate of Y is much greater than W. By the theory of allometry, this means that the biomass of each species is strongly diversified. For the ZY-prolificacy parameter ϵ_1, it is not obvious that the prolificacy hypothesis should or should not apply since Y, Z are competitors rather than chain predators. It can range from very small to very large. However, for this paper we will assume the following.

Condition 2. *Asymmetric competitive prolific diversification condition:*

$$0 \ll b_2p_2 \ll b_1p_1 \ll r, \text{ equivalently, } 0 < \epsilon_1 \ll 1 \ll \frac{1}{\zeta}.$$

What is left open is the relative maximal birthrate ϵ_1/ϵ_2 between the competitor Z and the super predator W. In fact, it is this relative rate ϵ_1/ϵ_2 that will be used as the effective bifurcation parameter for this paper.

4.1. Joint yz Weakness.

Conditions 1, 2 make the x equation the ζ-fast subsystem and the yzw equations the ζ-slow subsystem. The next condition guarantees that the flow of the ζ-slow subsystem will not escape from the stable portion of the x-nullcline, referred to loosely as being invariant. In the case of the xy-subsystem, for the y-adjusted capacity to be invariant (non-escaping) it requires the predator to be weak. However, having weak y and z individually is not enough for the invariance of the yz-adjusted x-capacity state. The stronger condition is introduced below, referred to as the joint yz-weakness condition.

Because the nontrivial nullclines of both y and z are parallel planes: $g(x, y, 0) = 0, h(x) = 0$ giving rise to $x = x_{\text{ynl}} = \beta_1\delta_1/(1-\delta_1), x = x_{\text{znl}} = \beta_2\delta_2/(1-\delta_2)$. We can conclude right away that

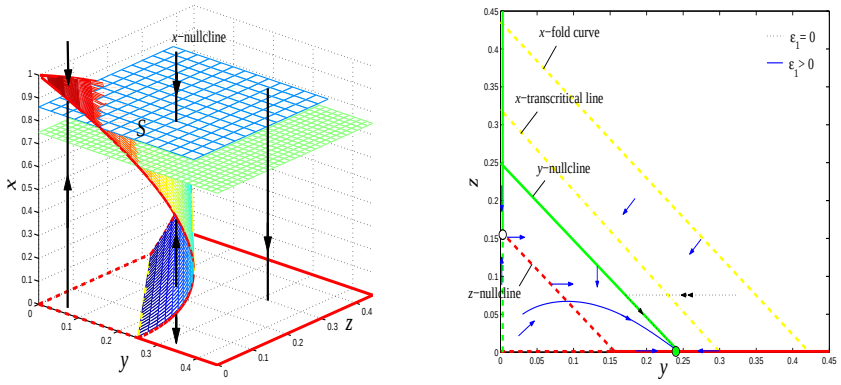

(a) (b)

FIGURE 2. (a) A 3-d view of the nullcline surfaces is shown. The stable branches of the x-nullcline are outlined in solid bold and unstable branches by dashed bold. Vertical phase lines are for the x-fast flows. The parallel planes are for the y-nullcline and z-nullcline surfaces for which for which both y, z are weak. (b) A reduced 2-d phase portrait view. The outermost dotted line is the crash-fold projection – any solution curve that touches this line will crash down to the trivial x nullcline, $x = 0$. A case of non-competitive z is shown in which z declines in part of the growing region of y. Solid vector field and curve for a perturbed case $\epsilon_1 > 0$ and dotted curves for ϵ_1-singular orbits. Both give the same z-extinction scenario.

no coexisting xyz-equilibrium state exists if $x_{\text{ynl}} \neq x_{\text{znl}}$, the phenomenon of Competition Exclusion Principle mentioned in the introduction. We will assume this inequality hold generically for the system.

For the singularly perturbed xyz-system, the attracting, nontrivial, slow manifold is part of the x-nullcline surface $f(x, y, z) = 0$ for which $f_x(x, y, z) < 0$, the yz-adjusted carrying capacity of x. For any point of the surface, the x value must decrease with any increase in either y or z (or both). We denote this surface $\mathcal{S}$ and its projection onto the yz-plane D for later usage, see Fig.3(b). Similar to the 1-dimensional crash-fold point $(x_{\text{xfd}}, y_{\text{xfd}})$ of the xy system, a joint crash-fold point develops at a given pair of (y, z) if at (y, z) there is an adjusted capacity x which disappears upon any small increase either in y or z. By a typical analysis of singular perturbation, the increase of a singular orbit over the crash-fold of $\mathcal{S}$ causes the singular orbit to crash in the prey x to zero.

The set of these crash-fold points is a curve whose y-coordinate and z-coordinate are reciprocal in relation: increasing the z-predation pressure only requires a smaller amount of predator y to crash the prey, and vice versa. Denote the crash fold points similarly by $(x_{\text{xfd}}, y_{\text{xfd}}, z_{\text{xfd}})$. The set of all crash folds points is part of the boundary of the capacity surface $\mathcal{S}$ and is determined by $f(x, y, z) = 0, f_x(x, y, z) = 0$.

Condition 3. *The joint yz-weak condition: The y-nullcline plane $x = x_{\text{ynl}}$ lies above the crash-fold curve $(x_{\text{xfd}}, y_{\text{xfd}}, z_{\text{xfd}})$ and analogously the z-nullcline plane $x = x_{\text{znl}}$ lies above the crash-fold curve as well.*

Recall that y is weak if $x_{\text{ynl}}|_{\{z=0\}} > x_{\text{xfd}}|_{\{z=0\}}$ and z is weak if $x_{\text{znl}}|_{\{y=0\}} > x_{\text{xfd}}|_{\{y=0\}}$. Thus the joint yz-weak condition implies individual weakness but the converse is not necessarily true. The joint yz-weakness condition can be expressed explicitly as follows

$$\min\{x_{\text{ynl}}, x_{\text{znl}}\} = \min_{i=1,2}\left\{\frac{\beta_i\delta_i}{1-\delta_i}\right\} > \max_{i=1,2}\left\{\frac{1-\beta_i}{2}\right\} = \max\{x_{\text{xfd}}|_{\{y=0\},\{z=0\}}\}. \tag{5}$$

The derivation can be found in [1]. We note that Condition 3 simply implies that with $w = 0$ the xyz-subsystem is governed by the Competition Exclusion Principle: the xy-equilibrium point is globally attracting if $x_{\text{znl}} > x_{\text{ynl}}$, i.e. z goes to extinction because it is not competitive for requiring a greater amount of the prey than y does to grow. Similarly, the xz-equilibrium point is globally attracting if $x_{\text{znl}} < x_{\text{ynl}}$. We will assume the former for the main result of this paper, i.e. *without w, the only asymptotic state is the xy-equilibrium point.*

4.2. **Dimension Reduction.** In order to apply singular orbit analysis, a thorough understanding of the nullclines is necessary. Here, we aim to reduce the system by showing we just need to consider the x-nullcline solid. The nontrivial x-nullcline $f(x, y, z) = 0$, its crash-fold, stable, and unstable branches are the same for the full system as for its xyz-subsystem because w does not directly interact with x. As before, the stable branch of the x-nullcline is denoted as $\mathcal{S}$.

Joint weakness implies that everywhere along the crash fold curve, none of the predators can grow. In other words, once a ζ-slow singular orbit starts on the predator-adjusted carrying capacity $\mathcal{S}$, the orbit will stay on the surface because along the crash-fold boundary y, z are in decline, preventing x from crashing. Therefore the surface $\mathcal{S} \cap \{w = 0\}$ is invariant for the ζ-slow yz-subsystem. With the introduction of w predation, y must be in a steeper decline near the x-fold than without (as $g_w(x, y, w) < 0$). By the same reasoning crashing in x is impossible. Hence the solid $\mathcal{S}$ is invariant for the full ζ-slow yzw-system.

Mathematically, S is defined by $f(x, y, z) = 0, f_x(x, y, z) < 0$. Because of the hyperbolicity $f_x(x, y, z) < 0$, variable x can be solved by the Implicit Function Theorem as a function $q(y, z)$ from $f(x, y, z) = 0$ with (y, z) from the same set D that is bounded by the y, z axes and the projected x-crash-fold boundary in the yz-plane. The quantity $q(y, z)$ is the unique, yz-adjusted carrying capacity of the prey. Also, the function q is decreasing in both y and z (see [1] for analytical justification) because any additional predatory pressure depresses the adjusted prey carrying capacity further.

On the trivial x-slow manifold $x = 0$, the transcritical points for the full 4-species web remain the same as for the xyz-web subsystem. All ζ-singular orbits must cross it and jump to the solid $\mathcal{S}$ at some x-outbreak PDLS points. Therefore, all nontrivial ζ-singular orbits eventually settle down in the invariant solid $\mathcal{S}$. And we only need to consider the 3-dimensional yzw-slow system in $\mathcal{S}$. A dimension reduction is now obtained.

Proposition 4.1. *Under the joint yz-weak condition the predator-adjusted prey capacity manifold $\mathcal{S}$ attracts all singular orbits and it is invariant for the yzw-slow subsystem.*

The ζ-slow yzw-system in $\mathcal{S}$ can now be expressed explicitly as follows:

$$\begin{cases} \dfrac{dy}{dt} = y\left(\dfrac{q(y,z)}{\beta_1 + q(y,z)} - \dfrac{w}{\beta_3 + y} - \delta_1\right) = yg(q(y,z), y, w) \\ \dfrac{dz}{dt} = \epsilon_1 z\left(\dfrac{q(y,z)}{\beta_2 + q(y,z)} - \delta_2\right) = zh(q(y,z)) \\ \dfrac{dw}{dt} = \epsilon_2 w\left(\dfrac{y}{\beta_3 + y} - \delta_3\right) = wk(y) \end{cases} \tag{6}$$

5. Qualitative Properties of Nullcline Surfaces

Having achieved the dimension reduction to the solid $\mathcal{S}$, we now begin our singular orbit analysis by first describing the y, z, w nullclines holistically and geometrically. Most mathematical technicalities can be bound in [1].

5.1. w **and** z **Nullclines.** The nontrivial w nullcline for the reduced system (6) is the simplest: $k(y) = 0$ giving rise to $y = y_{\text{wnl}} = \beta_3\delta_3/(1-\delta_3)$, a plane parallel to the zw-plane in $\mathcal{S}$. Thus, recovery or decline in w takes place depending entirely on the size of y. If $y < y_{\text{wnl}}$, w decreases because of insufficient food supply; on the other side of the nullcline, w increases.

The nontrivial z nullcline is slightly more complicated: $h(q(y,z)) = 0$ gives $q(y,z) = x_{\text{znl}} = \beta_2\delta_2/(1-\delta_2)$. It is a plane parallel to the w-axis, through a curve $q(y,z) = x_{\text{znl}}$ on the yz-plane. It defines the y competition-adjusted xz equilibrium state. The z nullcline is also the state where z either starts rebounding or declining depending on whether or not the competition strength from y weakens ($\dot{y} < 0$) or intensifies ($\dot{y} > 0$). We already know the function q decreases in both y and z. Hence to maintain a constant level $q(y,z) = x_{\text{znl}}$, y and z must behave in opposite manner along this curve: an increase in y must be counter-balanced by a decrease in z. Therefore, the curve has negative slopes everywhere in $\mathcal{S}$.

5.2. y **Nullcline.** The most complex nullcline is the nontrivial y-nullcline surface, $g(q(y,z), y, w) = 0$. It is more simply expressed when solved for w:

$$w := p(y,z) = \left(\frac{q(y,z)}{\beta_1 + q(y,z)} - \delta_1\right)(\beta_3 + y). \tag{7}$$

Biologically, the nullcline is the capacity state for y in $\mathcal{S}$, adjusted in the presence of predation by w and competition from z. Two special cases of this nullcline are well-known. First, when $w = 0$, it is a curve in $\mathcal{S}$ for the xyz-web case analyzed above. The other special case is the xyw-chain with $z = 0$, which is the classic Rosenzweig-MacArthur food chain [27]. It is also a curve in $\mathcal{S}$, see [7, 8, 9, 10]. Periodic and chaotic oscillations occur only if w is efficient so that the y-nullcline curve on $\mathcal{S}$ develops a crash-fold point. The y-crash-fold points are guaranteed by a similar but z-mediated condition (see [1] for a proof).

Condition 4. *The w is efficient, i.e.* $\max\left\{\frac{1-\beta_i}{2}\right\} < \min\left\{\frac{\beta_i\delta_i}{1-\delta_i}\right\}$, $\beta_3 < \frac{(\beta_1+1)^3}{\beta_1}\left(\frac{1}{\beta_1+1} - \delta_1\right)$.

Notice that the first set of the condition is the joint yz-weakness condition, but the second set says the relative half-saturation constant of w should be small, a requirement for predatory efficiency, consistent with the efficiency definition for y earlier. In this paper we further require

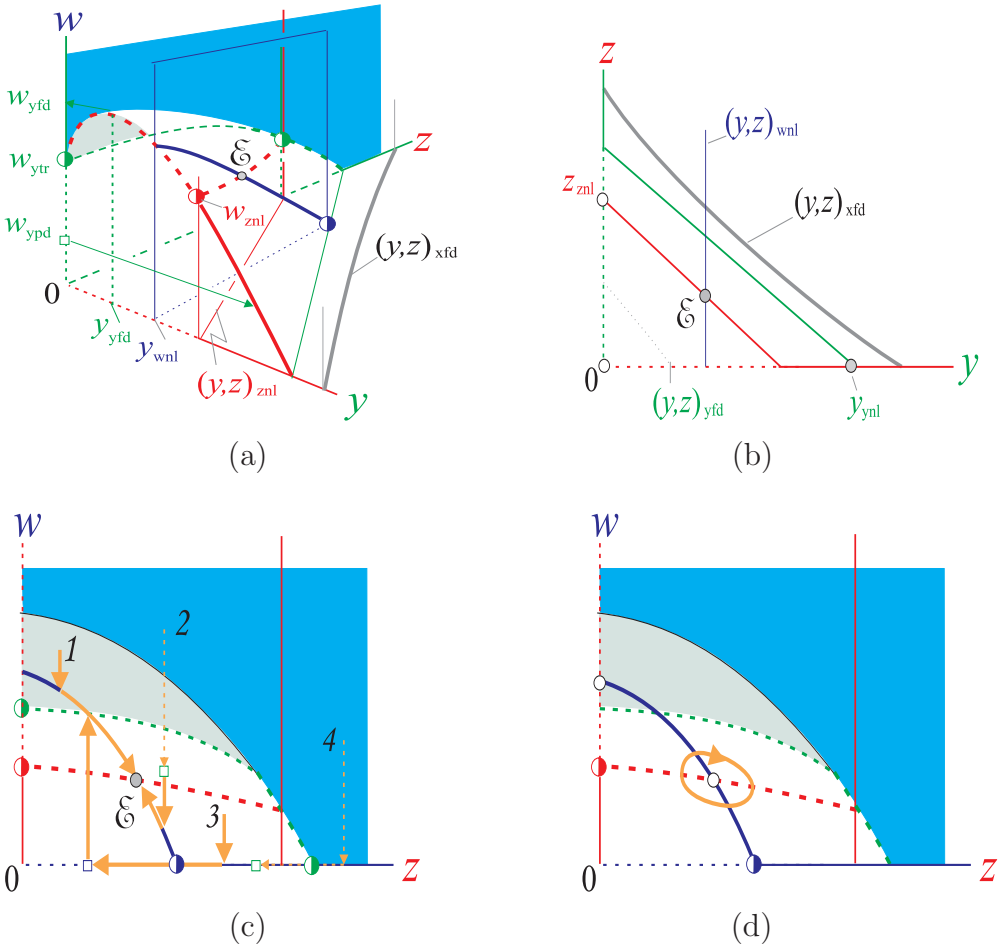

FIGURE 3. (a) Nullcline surfaces inside the x-nullcline solid $\mathcal{S}$. Stable branches of the y-nullcline are shaded for the trivial branch $y = 0$ and left blank for the nontrivial part $w = p(y, z)$. The unstable branches are left blank on $y = 0$ and shaded slightly for $w = p(y, z)$ between the y crash-fold and the transcritical curve. Vertical planes are the nontrivial w and z nullcline surfaces respectively. The case of Condition 6 is shown for which the w-nullcline surface intersects the nontrivial stable branch of the y-nullcline only. Half-filled circles are transcritical points, and squares PDLS jump points. (b) The yz-projection view of (a). Left to the y-crash-fold curve, the y-nullcline surface is unstable, and to its right, it is stable. The y-nullcline surface is bounded by the coordinate axes and the y-boundary curve, second right. The yz, yw nullclines intersect at the equilibrium point $\mathcal{E}$. (c) The zw-projection view of (a) for the case that w has the faster time scale than z does. The vertical phase curves are the w-fast orbits and the horizontal phase curves are the z-slow orbits, all eventually converging to the equilibrium point $\mathcal{E}$. (d) The same structure as (c) except that as the time scale of z increases against that of w, a y-slow cycle is born through a Hopf bifurcation at $\mathcal{E}$.

w to be weak by the following condition. That is, although it is possible for w to crash y but in actuality it cannot because of its relative high death rate.

Condition 5. *The w is weak, i.e.* $y_{\rm wnl}|_{\{z=0\}} = \frac{\beta_3\delta_3}{1-\delta_3} > y_{\rm yfd}|_{\{z=0\}}$.

Here the parameter value $y_{\rm yfd}$ is implicitly defined by the w-efficiency condition. Notice that this condition leads to one important aspect of the main result, that is, *in the absence of z, the xyw food chain with the chain prolific time diversification has the xyw-equilibrium point as the only global asymptotic state*, see the yw-section ($z = 0$) of Fig.3(a). There is no xyw cycles, chaotic or otherwise. The necessary condition for it to behave otherwise is for w to be strong ([7, 8, 9, 10]).

The effective region of the y-nullcline requires $w = p(y, z)$ to be positive, which in turn imposes a constraint on variable y, z. That $w = p(y, z) > 0$ holds precisely in the triangular shaped region bounded by the y, z axes and its intersection with $w = 0 : g(q(y, z), y, 0) = 0$. From the expression of $w = p(y, z)$ above, we see that $p(y, z) > 0$ if and only if $q(y, z)/(\beta_1 + q) - \delta_1) > 0$. This condition solves as $q(y, z) > \beta_1\delta_1/(1 - \delta_1) = x_{\rm ynl}$. As q decreases in both y and z, both variables must be smaller than at the boundary $q(y, z) = x_{\rm ynl}$. Hence the domain for $p(y, z) > 0$ is given as $\Delta := \{(y, z) \in \mathcal{S} : (y, z)$ in the first quadrant left of the y-nullcline curve on $w = 0\}$. Alternatively, for a fixed competition intensity of z, and an elevated predatory pressure $w > 0$, the adjusted equilibrium y level must be lower than what would be if the top-predation is absent, $w = 0$.

The topography of the surface can be understood holistically as well. For fixed y in Eq.(7), increasing z decreases $q(y, z)$, the steady x supply in $\mathcal{S}$. This decreases the quantity $q(y, z)/(\beta_1 + q(y, z))$, which represents the per-capita catch of the prey x by y. Thus, the increased z decreases $p(y, z)$. In practical terms, if y is fixed and the competition level of z is increased, then the system requires a smaller amount of predatory pressure from w to separate the increasing phase $\dot{y} > 0$ from the decreasing phase $\dot{y} < 0$ of y. Either way, the y-section curves on the surface are all decreasing in z, all the way down to $w = 0$ on the boundary of Δ.

It is slightly more complex to visualize the z-section curves on the surface. We begin with the special case $z = 0$. By the w-efficiency condition above, the y nullcline has a fold point, and this fold point is continued as a curve as z increases. This y-fold curve separates the y-nullcline into the w-adjusted capacity state and the y-threshold state. The former is stable and the latter is unstable for the y-dynamics. The stable branch is a monotone decreasing function of w: fixed at a greater w depletes the steady supply y. The unstable, threshold branch is a monotone increasing function of w: fixed at a greater w requires a greater threshold amount of y for y to increase. The two branches coalesce at the crash-fold.

The y-crash-fold curve decreases in w as z increases. This is because for an increased value $z > 0$, the competition makes fewer resource available for y, and makes y more vulnerable. Hence it takes a smaller w amount to crash y. In other words, as z increases, both y and w decrease along the fold curve. A more detailed justification can be made as follows. Since the w-nullcline, $y = y_{\rm wnl} = \beta_3\delta_3/(1 - \delta_3)$, contains parameter δ_3 which is independent of the parameters that defines the y nullcine surface, we can use it to sweep the surface to determine the structure of the crash-fold. Now if $y = y_{\rm wnl}$ was exactly at the crash-fold $y_{\rm yfd}$ for a given z, then for a larger

z, the corresponding yw-dynamics should be weaker in w. Since the w-nullcine $y = y_{\text{wnl}}$ remains the same, then for w to be weaker the y-crash-point must drop lower than y_{wnl} so that w cannot dynamically crash it. What about the crash density w_{yfd}? Since increasing z decreases w along the surface, the corresponding crash density w_{yfd} is smaller than the w value for the original z at the smaller crash density y_{yfd}. Since the crash density w_{yfd} at the original z is the largest w value along the z-section, the crash density w_{yfd} for the larger z must be smaller than that for the original smaller z. Hence, we can conclude that the y-crash-fold decreases not only in the w-coordinate w_{yfd} but also in the y-coordinate y_{yfd} when z increases, see Fig.3.

6. Coexisting Cycle via Hopf Bifurcation

Finally, it is left to describe the intersections of these nullcline surfaces. The intersection of the w-nullcline surface $y = y_{\text{wnl}}$ with the y-nullcline $w = p(y, z)$ is a monotone decreasing curve of w in z as we have already derived this property for all y-section curves on the surface $w = p(y, z)$. It goes from the section $z = 0$ to $0 = w = p(y_{\text{wnl}}, z)$ with $z > 0$. The intersection of the z-nullcline $x = q(y, z) = x_{\text{znl}}$ with the y-nullcline surface is $w = p(y, z) = (x_{\text{znl}}/(\beta_1 + x_{\text{znl}}) - \delta_1)(\beta_3 + y)$ which is, obviously, a monotone increasing line in y. With the constant supply $x = q(y, z) = x_{\text{znl}}$, increasing z decreases y, which in turn decreases $w = p(y, z) = (x_{\text{znl}}/(\beta_1 + x_{\text{znl}}) - \delta_1)(\beta_3 + y)$. So the intersection curve is a decreasing function of w as z increases. In practical terms, increasing y decreases z on the fixed supply level $x = x_{\text{znl}}$ of x. This improves the status of predator y. As a result, it would take a greater amount of the top-predator w to flip y from growing ($\dot{y} > 0$) into declining ($\dot{y} < 0$). However, unlike the w-nullcline intersection for which $y = y_{\text{wnl}}$ is fixed, it goes from $z = 0$ to $y = 0$ with increasing z and decreasing y. Therefore, when $y_{\text{znl}}|_{\{z=0\}}$ is greater than both $y_{\text{wnl}}|_{\{z=0\}} = y_{\text{wnl}}$ and y_{yfd}, the w and z nontrivial nullcines must intersect on the stable nontrivial y-nullcline surface because they eventually exchange positions in the y variable with the former $y = y_{\text{wnl}} > 0$ when reaching the boundary of $w = p(y, z)$ and $y = 0$ for the latter (see Fig.3(a,b)). Because of the monotonicity of the z-nullcline in y, the intersection is unique. The intersection is the unique $xyzw$ equilibrium point of the system, denoted by $\mathcal{E}$. Thus we assume the following:

Condition 6. *Equilibrium coexistence condition:* $y_{\text{wnl}} = \frac{\delta_3\beta_3}{1-\delta_3} < y_{\text{znl}}|_{\{z=0\}} = (1-\frac{\beta_2\delta_2}{1-\delta_2})(\beta_1+\frac{\beta_2\delta_2}{1-\delta_2})$.

Note that this condition means that although z is not competitive against y with $w = 0$ for requiring a greater amount of x to grow (resulting $y_{\text{znl}}|_{\{z=0\}} < y_{\text{ynl}}|_{\{z=0\}}$, Fig.2(b), Fig.3(b)), but the corresponding minimal amount of y, $y_{\text{znl}}|_{\{z=0\}}$, for it to happen is greater than the minimal amount of y, y_{wnl}, required by w for w to grow. Because of this extra help from w, it is possible for z to coexist at the w-induced equilibrium state $\mathcal{E}$. Also, since the y-crash-fold decreases in y as z increases and $y = y_{\text{wnl}} > y_{\text{yfd}}$ is a constant, the y-crash-fold always lies left the w-nullcline (Fig.3(a,b)). Therefore, the $xyzw$-equilibrium point $\mathcal{E}$ is always on the stable part of the y-nullcline under Condition 6. Fig.3 has incorporated all the descriptions given above. All analytical justifications can be found from [1].

We are now ready to state part of the main result.

Theorem 1. *Assume the Conditions 1 – 6. Then for each $0 < \epsilon_2 \ll 1$, there is a value $\epsilon_1 = \theta(\epsilon_2)$ such that a pair of eigenvalues of the linearization at $\mathcal{E}$ crosses the imaginary axis.*

Proof. As concluded above, Conditions 1 - 6 guarantee the existence of the equilibrium point and force the equilibrium point to be on the stable portion of the y-nullcline. From Conditions 1 and 2, for some neighborhood U of the equilibrium point, all singular orbits will be attracted into the solid $\mathcal{S}$ because x has the fastest time scale. Because the next fastest time scale belongs to y, then there is some refinement of U, U', in which all singular solutions go onto the stable part of the y-nullcline. By Fenichel's geometric theory of singular perturbation, the invariant y-slow manifold in a compact neighborhood near $\mathcal{E}$ persists for small $0 < \epsilon_2 \ll 1$ treating $0 < \epsilon_1/\epsilon_2 \ll 1$ as a new time scale independent of ϵ_2. On this 2-dimensional manifold the yzw-system can be projected onto the zw-plane. In a neighborhood of the $\mathcal{E}$, the zw-phase plane looks qualitatively like Fig.3(c,d). To analyze the eigenvalues we adopt a more qualitative approach. More specifically, the linearized equation can be written as follows $\dot{u} = \epsilon_1 c_1(au + v), \dot{v} = -\epsilon_2 c_2(bu + v)$ with $(u, v) = (0, 0)$ corresponding to the equilibrium point $\mathcal{E}$ in (z, w). Here, a, b, c_1, c_2 are constants satisfying the following conditions. Because u-equation's right side is the linearization of the vector field $\epsilon_1 zh$ restricted on the y-slow manifold, the u-nullcline $au + v = 0$ is precisely the tangent line to the z-nullcline at $\mathcal{E}$. Therefore, it has negative slope, forcing $a > 0$. Exactly the same argument results in $b > 0$. In addition, the relative position of these u-, v-nullclines preserves that of the z-, w-nullclines, we must have $b > a > 0$ because w decreases faster on the w-nullcline than on the z-nullcline. Since $\dot{z} > 0$ for points above the z-nullcline, which include points of large w because a significant presence of w enhances the competitiveness of z. Since the linearization in terms of u mirrors the same qualitative property, we must have the constant $c_1 > 0$ to be positive. Exactly the same argument leads to $c_2 > 0$. See Fig.3(c,d) for an illustration. Since ϵ_i and $\epsilon_i c_i$ have the same order of magnitude, we will let $\epsilon_i := \epsilon_i c_i$ for simpler notations in the following calculation. Now the eigenvalues $\lambda_{1,2}$ of the linear uv-system are

$$\lambda_{1,2} = \frac{1}{2}[\epsilon_1 a - \epsilon_2 \pm \sqrt{(\epsilon_1 a - \epsilon_2)^2 - 4\epsilon_1\epsilon_2(b - a)}].$$

We now see easily that the eigenvalues are pure imaginary at $\epsilon_1 a - \epsilon_2 = 0$, and their real parts change from negative to positive as ϵ_1 increases above ϵ_2/a. This completes the proof. □

Note that we did not verify all the conditions of the Hopf Bifurcation Theorem. The omitted part addresses whether the limit cycle is stable or unstable for which the computations are extremely complicated. For this reason we will rely on numerical simulation below.

7. Period-Doubling Bifurcation — Numerical Simulation

We now pick and fix parameter values that satisfy all the Conditions 1 – 6 and change only the relative ZW prolificacy parameter ϵ_1/ϵ_2. The chaotic attractor of Fig.4(a) is produced for these parameter values:

$$\begin{array}{ccc} \zeta = .1 & \epsilon_1 = .1 & \epsilon_2 = .01 \\ \beta_1 = .3 & \beta_2 = .57 & \beta_3 = .2 \\ \delta_1 = .6 & \delta_2 = .52 & \delta_3 = .54 \end{array}$$

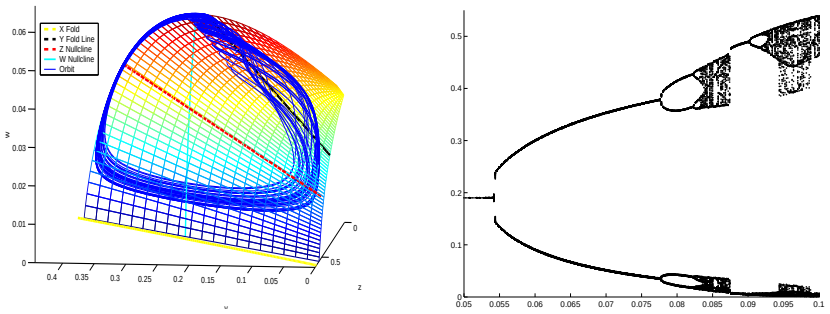

(a) (b)

FIGURE 4. (a) A phase plot of the attractor at $\epsilon_1 = 0.1$. (b) A bifurcation diagram in the variable ϵ_1. It is generated by running a numerical simulation for each parameter value of ϵ_1 and plotting a point in z whenever the solution curve crosss the z-nullcline from either up or down direction. Thus the simple periodic orbit from the Hopf bifurcation registers two points on the plot.

Fig.4(b) is a bifurcation diagram with parameter ϵ_1 ranging from 0.05 to 0.1 (equivalent with ϵ_1/ϵ_2 from 5 to 10). The first bifurcation point is the Hopf bifurcation from the equilibrium point. It occurs around $\epsilon_1 = 0.053$ by AUTO2000. Subsequent bifurcations are the type of period doubling between $\epsilon_1 = 0.078$ and $\epsilon_1 = 0.083$. Other notable features include a 3 period cycle around $\epsilon_1 = .0853$, and the onset of chaos which stays at a discernable distance away from the extinction edge $z = 0$.

REFERENCES

1. Bockelman, B., B. Deng, E. Green, G. Hines, L. Lippitt, and J. Sherman, *Chaotic coexistence in a top-predator mediated competitive exclusive web,* J. Dyn. Diff. Eq. **16**(2004), pp.1062–1092.
2. Armstrong, R.A. and R. McGehee, *Competitive exclusion,* Amer. Naturalist, **115**(1980), pp.151–170.
3. Bonet, C., *Singular perturbation of relaxed periodic orbits,* J.D.E., **66**(1987), pp.301–339.
4. Calder III, W.A., *An allometric approach to population cycles of mammals,* J. Theor. Biol., **100**(1983), pp.275-282.
5. Calder III, W.A., *Ecological scaling: mammals and birds,* Ann. Rev. Ecol. Syst., **14**(1983), pp.213-230.
6. Deng, B., *Glucose-induced period-doubling cascade in the electrical activity of pancreatic β-cells,* J. Math. Bio., **38**(1999), pp.21–78.
7. Deng, B., *Food chain chaos due to junction-fold point,* Chaos, **11**(2001), pp.514–525.
8. Deng, B. and G. Hines, *Food chain chaos due to Shilnikov orbit,* Chaos, **12**(2002), pp.533–538.
9. Deng, B. and G. Hines, *Food chain chaos due to transcritical point,* Chaos, **13**(2003), pp.578–585.
10. Deng, B., *Food chain chaos with canard explosion,* Chaos, **14**(2004), pp.1083–1092.
11. Eckhaus, W., *Relaxation oscillations including a standard chase on French ducks,* in Asymptotic analysis II, Springer Lecture Notes Math. **985**(1983), pp.449–494.
12. Fenichel, N., *Geometric singular perturbation theory for ordinary differential equations*, J. Diff. Eq., **31**(1979), pp.53–98.
13. Gilpin, M.E., *Spiral chaos in a predator-prey model,* Amer. Naturalist, **113**(1979), pp.306–308.
14. Holling, C.S., *Some characteristics of simple types of predation and parasitism,* the Canadian Entomologist, **91**(1959), pp.385–398.

15. Hogeweg, P. and B. Hesper, *Interactive instruction on population interactions,* Comput. Biol. Med., **8**(1978), pp.319–327.
16. Koch, A.L., *Competitive coexistence of two predators utilizing the same prey under constant environmental conditions,* J. Theoret. Biol., **44**(1974), pp.373–386.
17. Kooi, B.W. and S.A.L.M. Kooijman, *Invading species can stabilize simple trophic systems,* Ecol. Modelling, **133**(2000), pp.57–72.
18. Liu, W., D. Xiao, and Y. Yi, *Relaxation oscillations in a class of predator-prey systems,* J. Diff. Eq. **188**(2003), pp.306–331.
19. Loladze, I., Y. Kuang, J.J. Elser, and W.F. Fagan, *Competition and stoichiometry: coexistence of two predators on one prey,* Theor. Pop. Bio. **65**(2004), pp.1-15.
20. Lotka, A.J., *Elements of Physical Biology,* Williams and WWilkins, Baltimore, Md., 1925.
21. May, R.M., *Simple mathematical models with very complicated dynamics,* Nature **261**(1976), pp.459–467 .
22. Mishchenko, E.F., Yu.S. Kolesov, A.Yu. Kolesov, and N.Kh. Rozov, Asymptotic Methods in Singularly Perturbed Systems, Monographs in Contemporary Mathematics, Consultants Bureau, New York, 1994.
23. Muratori, S. and S. Rinaldi, *Low- and high-frequency oscillations in three-dimensional food chain system,* SIAM J. Appl. Math., **52**(1992), pp.1688–1706.
24. O'Malley, Jr., R.E., Introduction to Singular Perturbations, Academic Press, New York, 1974.
25. Pontryagin, L.C., *Asymptotic behavior of solutions of systems of differential equations with a small parameter at higher derivatives,* Izv. Akad. Nauk. SSSR Ser. Math. **21**(1957), pp.605-626 (in Russian).
26. Rai, V., *Chaos in natural populations: edge or wedge?* Ecological Complexity, **1**(2004), pp.127–138.
27. Rosenzweig, M.L. and R.H. MacArthur, *Graphical representation and stability conditions of predator-prey interactions,* Amer. Naturalist, **97**(1963), pp.209–223.
28. Schecter, S., *Persistent unstable equilibria and closed orbits of a singularly perturbed equation,* J. Diff. Eq., **60**(1985), pp.131–141.
29. Verhulst, P.F., *Notice sur la loi que la population suit dans son accroissement,* Corr. Math. et Phys. **10**, pp.113-121(1838).
30. Volterra, V., *Fluactuations in the abundance of species, considered mathematically,* Nature, **118**(1926), pp.558–560.
31. Waltman, P., Competition Models in Population Biology, SIAM, Philadelphia, 1983.

Department of Mathematics, University of Nebraska-Lincoln, NE 68588. Correspondence Email: bdeng@math.unl.edu